2025 International Symposium on Nonlinear Theory and Its Applications,
NOLTA2025, Naha city, Okinawa, Japan, October 27-31, 2025

Koopman Mode Decomposition of Transient Weather Dynamics: A Case Study on Short-Term Humidity Ratio Data

Zhicheng Zhang†, Yoshihiko Susuki†, and Atsushi Okazaki‡

†Department of Electrical Engineering, Kyoto University
Katsura, Nishikyo-Ku, Kyoto 615-8510, Japan

‡Institute of Advanced Academic Research, Center for Environmental Remote Sensing, Chiba University
1-33 Yayoi-cho, Inage, Chiba, Chiba, 263-0022, Japan

Email: zhang.zhicheng.2c@kyoto-u.ac.jp; susuki.yoshihiko.5c@kyoto-u.ac.jp; atsushi.okazaki@chiba-u.jp

Abstract—In this study, we take the short-term weather simulations into account by analyzing time series data measured from the humidity ratio field, where the resultant system is governed by transient dynamics. By virtue of Koopman Mode Decomposition (KMD) and its associated numerical method, Sparsity-Promoting Dynamic Mode Decomposition (SPDMD), we effectively capture the dominant transient modes characterized by a warm bubble-like pattern, providing a low-dimensional linear representation of the weather system. Furthermore, we balance accuracy and model complexity by adjusting the sparsity weight.

1. Introduction

The variability to identify dominant modes in weather dynamics is crucial for improving short-term weather forecasting, particularly for extreme events such as heavy rainfall [1]. In recent years, operator-theoretic approaches, especially Koopman mode decomposition (KMD) [2] and its numerical counterpart–dynamic mode decomposition (DMD) [3]—have been successfully applied in fluid dynamics [4], power systems [5], and climate science [6] to extract dominant modes. Building on these achievements [2], this study utilizes applied Koopmanism to weather systems, with a particular focus on sparsity-promoting DMD (SPDMD) [7], which penalizes an ℓ_1 norm on the amplitudes to balance the accuracy and model complexity.

In contrast to the climate system, which relies on long-term data and enjoys the steady-state behavior [6], the weather system is often governed by transient dynamics using short-term snapshots. In this study, we primarily leverage SPDMD to explore the dominant modes in transient weather dynamics, referred to as *transient modes*, capturing *warm bubble-like patterns* in the evolution of weather simulations (e.g., Scalable Computing for Advanced Library Environment, SCALE [8]) acting on the specific humidity observable data space. These bubble-like patterns commonly appear in convection-permitting weather model, where rising warm air from cumulonimbus clouds interacts with descending cumulus clouds [1]. Notice that in such weather models, the humidity ratio is closely related to precipitation, as it quantifies the amount of water vapor per kilogram of dry air. The warmer the air, the more moisture it can hold, and when this air rises and cools, the excess moisture may condense, leading to precipitation event. Therefore, the humidity ratio plays a crucial role in evaluating whether rainfall will occur in weather prediction.

To this end, this study intends to provide an effective yet simple method to extract the warm bubble-like features (i.e., transient modes) in SCALE weather simulations of the humidity ratio data field, offering potential insights for short-term weather forecasting to prevent torrential rain.

2. Data Source and Methods

In this section, we emphasize that the data are measured from the SCALE weather simulation [8], specifically with respect to the humidity ratio data field. We briefly introduce DMD and its extension with the sparsity-promoting technique (i.e., SPDMD), e.g., see [3, Chapter 1] and [7].

2.1. Data source: Humidity Ratio Data Field

In this study, we focus on the SCALE weather simulation acting on the observable space in terms of the humidity ratio data field*, denoted as

$$\mathbf{y}_k = \mathtt{D}_{\mathtt{QV}}(k), \quad k = 0, 1, \ldots 120, \tag{1}$$

where k denotes the iteration step, with each iteration being 30 seconds, running a total of 3600 seconds (1 hour or 60 minutes) using SCALE simulations, and the data matrix $\mathtt{D}_{\mathtt{QV}} := \mathtt{data.QV} \in \mathbb{R}^{3880\times 121}$ quantifies the mass ratio of water vapor to total air pressure on the y-z plane, with y (horizontal) spanning 40 points at a 0.5 km resolution and z (vertical) consisting of 97 layers extending up to 20 km, consisting of $40 \times 97 = 3880$ grid points.

*The humidity ratio evolution in the SCALE simulation is accessible. For other data fields in SCALE simulations with SPDMD, refer to [9].

ORCID iDs First Author: 0000-0002-1548-4891, Second Author: 0000-0003-4701-1199, Third Author: 0000-0002-4598-0589

2.2. Method-I: Dynamic Mode Decomposition

Firstly, we briefly recall the DMD architecture [3, Chapter 1], which begins with the measurement of the system

$$\mathbf{y}_k = \mathbf{f}(\mathbf{x}_k), \tag{2}$$

where $\mathbf{x}_k$ represents the system state evolving within the state space $\mathcal{X} \subseteq \mathbb{R}^n$, and $\mathbf{y}_k \in \mathbb{R}^p$ denotes the measured output at time k, determined by the vector-valued observable function $\mathbf{f} : \mathcal{X} \to \mathbb{R}^p$, which may be nonlinear and possibly act in a high-or even infinite-dimensional space.

In general, a finite-length time series data snapshots $\{\mathbf{y}_k\}_{k=0}^N$, such as humidity ratio data source (1), can be directly sampled from (2) and compactly arranged as follows

$$\mathbf{Y} := [\mathbf{y}_0\ \mathbf{y}_1\ \ldots\ \mathbf{y}_{N-1}], \quad \mathbf{Y}' := [\mathbf{y}_1\ \mathbf{y}_2\ \ldots\ \mathbf{y}_N], \tag{3}$$

where $\mathbf{Y}, \mathbf{Y}' \in \mathbb{R}^{p\times N}$, $\mathbf{Y}'$ is a time shifted data matrix of $\mathbf{Y}$. Suppose that these data snapshots can be approximated by a discrete-time linear time-invariant system as follows

$$\mathbf{y}_{k+1} \approx A\mathbf{y}_k, \quad \Longrightarrow \quad \mathbf{Y}' \approx A\mathbf{Y}. \tag{4}$$

The best-fit matrix $A \in \mathbb{R}^{p\times p}$ is computed by $A = \mathbf{Y}'(\mathbf{Y})^\dagger$, where $(\cdot)^\dagger$ is the Moore-Penrose pseudoinverse. This minimizes the least-squares error of linear model (4), that is, $A \in \arg\min \|\mathbf{Y}' - A\mathbf{Y}\|_{\mathrm{F}}$, here $\|\cdot\|_{\mathrm{F}}$ is the Frobenius norm. However, for high-dimensional model, such an exact solution may be intractable for direct analysis.

In practice, it is more efficient to compute the reduced-order or projected matrix $\tilde{A} \in \mathbb{C}^{r\times r}$ of the full operator A in the subspace spanned by the left singular vectors U (i.e., the proper orthogonal modes). This is based on the fact that

$$\tilde{A} = \mathrm{U}^* A\mathrm{U} = \mathrm{U}^*\mathbf{Y}'\mathrm{V}\Sigma^{-1} \quad \Longleftarrow \quad A = \mathbf{Y}'\mathrm{V}\Sigma^{-1}\mathrm{U}^*, \tag{5}$$

which follows from singular value decomposition (SVD) of the data matrix $\mathbf{Y} = \mathrm{U}\Sigma\mathrm{V}^*$, where $\mathrm{U} \in \mathbb{C}^{p\times r}$, $\Sigma \in \mathbb{C}^{r\times r}$, and $\mathrm{V} \in \mathbb{C}^{N\times r}$, with $*$ denoting the conjugate transpose.

We derive reduced-order linear dynamical system of the form $\tilde{\mathbf{y}}_{k+1} = \tilde{A}\tilde{\mathbf{y}}_k$, while a high-dimensional model can be reconstructed as $\mathbf{y}_k = \mathrm{U}\tilde{\mathbf{y}}_k$. Applying eigen-decomposition $\tilde{A}w_j = \lambda_j w_j$ with a set of linear independent eigenvectors w_j and its associated eigenvalues λ_j, we obtain the DMD modes $\boldsymbol{\Phi}_r = \mathbf{Y}'\mathrm{V}\Sigma^{-1}W$ or equivalently $\boldsymbol{\Phi}_r = \mathrm{U}W$, where $\boldsymbol{\Phi}_r = [\boldsymbol{\phi}_1\ \ldots\ \boldsymbol{\phi}_r]$ and $W = [w_1\ \ldots\ w_r]$. The system evolution (4) can then be decomposed by

$$\mathbf{y}_k \approx \sum_{j=1}^{r} \boldsymbol{\phi}_j \lambda_j^k b_j, \quad \mathbf{y}_0 \approx \sum_{j=1}^{r} \boldsymbol{\phi}_j b_j, \tag{6}$$

where b_j are the modal amplitudes. Moreover, combining (2) and (6) implies that DMD provides a finite-dimensional approximation of the KMD[†]. Here, $\mathbf{y}_k$ denotes the flattened humidity ratio data on the y-z plane, and $\boldsymbol{\phi}_j$ is the spatial pattern of a single-frequency oscillation with temporal evolution $\lambda_j^k b_j$. The normal evolution is conducted by

$$a_k^{\text{mode } j} = \mathrm{Re}(e^{\mu_j k} b_j) \tag{7}$$

with $\mu_j = \log(\lambda_j)/\Delta t$, $\Delta t = 1$. If the absolute value (a.k.a., modulus) $|\lambda_j| = 1$ ($\lambda_j \neq 1$), then $a_k^{\text{mode } j}$ indicates a sustained oscillation. If $|\lambda_j| > 1$ (resp. $|\lambda_j| < 1$), it means the *transient mode* with growth (resp., decay) behavior.

In addition, (6) can be written as a compact form

$$\mathbf{Y} \approx \boldsymbol{\Phi}_r \mathrm{diag}(\mathbf{b}_r)\mathbf{V}_r, \tag{8}$$

where $\mathrm{diag}(\mathbf{b}_r)$ is the diagonal matrix form of the vector of amplitudes $\mathbf{b}_r := [b_1\ \ldots\ b_r]^\top \in \mathbb{C}^r$, $\boldsymbol{\Phi}_r$ contains the DMD spatial modes, and $\mathbf{V}_r$ is a Vandermonde matrix built from the eigenvalues λ_j representing the temporal evolution. The optimal solution $\mathbf{b}_r \in \arg\min \|\mathbf{Y} - \boldsymbol{\Phi}_r \mathrm{diag}(\mathbf{b}_r)\mathbf{V}_r\|_{\mathrm{F}}^2$ of (8) is obtained by solving a quadratic program [7, Section II].

2.3. Method-II: Sparsity-Promoting DMD

Previously, we derived the decomposition into the r spatial modes $\boldsymbol{\phi}_j$ with single frequencies characterized by λ_j. Here, to minimize the number of modes for low-order approximation of the data, we introduce the least-square error problem with ℓ_1 penalty (a.k.a., sparse constraint) as

$$\min_{\mathbf{b}_r \in \mathbb{C}^r} \|\mathbf{Y} - \boldsymbol{\Phi}_r \mathrm{diag}(\mathbf{b}_r)\mathbf{V}_r\|_{\mathrm{F}}^2 \quad \text{s.t.} \quad \|\mathbf{b}_r\|_1 \leq s, \tag{9}$$

where $\|\mathbf{b}_r\|_1 := \sum_{i=1}^r |b_i|$ is the ℓ_1 norm, and $s \in \mathbb{R}$ is the tuning parameter that can be adjusted to achieve a desired sparsity level. Note that the constrained convex program (9) can be recast into the regularized problem (10).

Jovanović *et al.* [7] proposed *sparsity-promoting* dynamic mode decomposition (SPDMD) that minimizes the regularized least-square error with additional ℓ_1-norm as

$$J_\gamma(\mathbf{b}_r) = \|\mathbf{Y} - \boldsymbol{\Phi}_r \mathrm{diag}(\mathbf{b}_r)\mathbf{V}_r\|_{\mathrm{F}}^2 + \gamma\|\mathbf{b}_r\|_1, \tag{10}$$

where $\gamma \geq 0$ is the weight to tune the sparsity level that balances the accuracy (i.e., the least-square error) and model complexity (i.e., the number of reduced amplitudes). SPDMD identifies a low-dimensional linear system to capture dominant modes while discarding weak features, extending the standard DMD algorithm to derive (8).

3. Experiment: Humidity Ratio Field

In this section, we mainly leverage the SPDMD to extract the transient modes of weather dynamics acting on the humidity ratio data fields, focusing on warm bubble-like patterns, where the data is provided in Subsection 2.1

In what follows, we consider the experiment of short-term SCALE simulations with $N = 51$ time steps or snapshots $\{\mathbf{y}_k\}_{k=0}^{50}$, leading to transient weather dynamics.

[†] As discussed in [5], the KMD takes the form $\mathbf{y}_k = \sum_{j=1}^{\infty} \lambda_j^k \boldsymbol{\varphi}_j(\mathbf{x}(0))\mathbf{v}_j$, where λ_j are the Koopman eigenvalues, $\boldsymbol{\varphi}_j$ denotes the Koopman eigenfunctions, and $\mathbf{v}_j$ represents the Koopman modes. By using finite-length time series data, KMD can be directly connected with DMD [2].

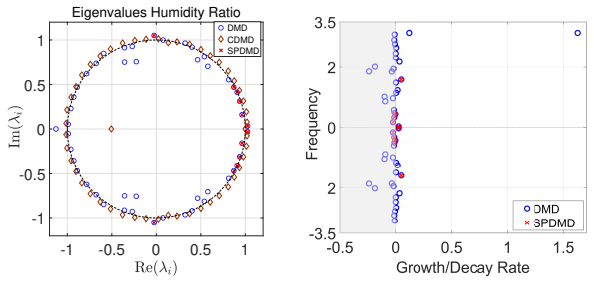

Figure 1: (left) the spectrum distribution of Koopman eigenvalues estimated with DMD (○), CDMD (♢), and SPDMD (×) methods for the data on humidity ratio field; (right) the horizontal axis represents the growth or decay rate, while the vertical axis corresponds to the frequency $\mathrm{Im}(\log\lambda_i)$, as estimated by DMD and SPDMD.

Hence, the dataset is represented as a *tall and skinny* matrix $\mathbf{Y} \in \mathbb{R}^{3880\times 51}$, which is high-resolution spatially and short-term temporally. The primary focus here still remains on capturing the transient modes (or warm bubble-like patterns) of the SCALE weather systems.

Fig. 1 and Table 1 mainly show the estimated eigenvalues with SPDMD. To assess the effectiveness of the SPDMD method, we also compare DMD and companion-based DMD (CDMD) [4] to estimate the eigenvalues, as shown on the left of Fig. 1. It is clear that the distribution of Koopman eigenvalues estimated with CDMD (♢) mostly lies outside the unit circle and shows less overlap (i.e., lower consistency) with those from DMD (○). Nevertheless, SPDMD (×) effectively aligns with the eigenvalue distribution identified by DMD and captures the dominant eigenvalues based on amplitude magnitude, as also verified on the right of Fig. 1 through the growth/decay rate and frequency. As shown in Table 1 for the SPDMD method, the identified eigenvalues denote transient states, providing a low-dimensional system representation. In particular, except for modes labeled 1 and 11, which correspond to eigenvalues with absolute values of $|\lambda_1| = 1.03 > 1$ and $|\lambda_{11}| = 1.05 > 1$, indicating *growth* modes, all other modes (i.e., $|\lambda_i| < 1$ for $i = 3, 5, 7, 9$) are *decay* modes.

To further examine the identified modes in Table 1, we present their temporal dynamics in Fig. 2, characterized by the normal evolution (7) for the SPDMD method. The top figure illustrates the evolution of the extracted modes, where modes 1 and 11 exhibit *growth* while oscillating at different slow and fast rates. The bottom figure simulates a longer time evolution, showing that the other four modes (labeled as $3, 5, 7, 9$) are decay modes with different periods, gradually decaying in time.

Mode i	Amp. $\lvert b_i\rvert$	Abs. $\lvert\lambda_i\rvert$	Eigval. λ_i	Period $\frac{2\pi}{\mathrm{Im}(\log\lambda_i)}$
1 (30)	0.1603	1.03	1.025 – 0.031i	204.97
3 (32)	0.0539	0.98	0.963 – 0.160i	38.17
5 (34)	0.0118	0.99	0.937 – 0.313i	19.50
7 (36)	0.0105	0.99	0.963 – 0.160i	14.74
9 (38)	0.0025	0.99	0.871 – 0.469i	12.72
11 (23)	0.0005	1.05	-0.025 – 1.051i	3.94

Table 1: The first 6 dominate modes estimated with the SPDMD method for the data on the humidity ratio field. These modes are ordered by their amplitudes.

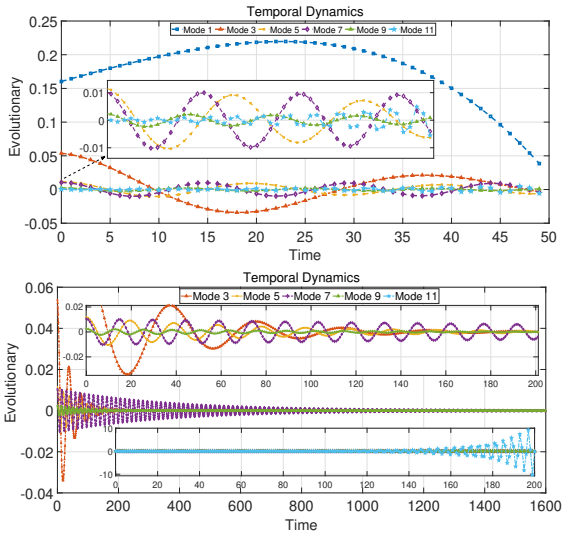

Figure 2: Normal evolution (7) for the SPDMD modes selected in Table 1. The top figure shows the evolution of all modes with zoom-in for clarity, and the bottom figure simulates a long-time with a focus on decay/growth behaviors.

As a counterpart to the temporal dynamics quantified by normal evolution and captured eigenvalues, the Koopman modes $\boldsymbol{\phi}_j$ computed by SPDMD reveal the corresponding spatial patterns in Fig. 3. Here, the element-wise of absolute values of $|\boldsymbol{\phi}_j|$ for $j = 1, 3, 5, 7, 9, 11$ are visualized. Compared to the original weather dynamics on the humidity ratio data field, shown in the animation in Subsection 2.1, it is clear that the all the SPDMD-based captured

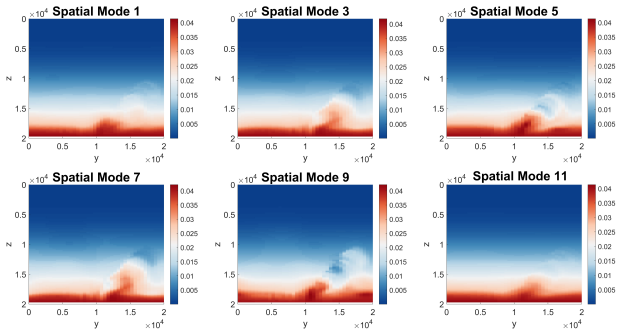

Figure 3: Spatial modes for the first 6 dominant Koopman modes selected with SPDMD from the transient weather simulations on the humidity ratio data. The element-wise absolute values of the Koopman modes $|\boldsymbol{\phi}_j|$ are visualized.

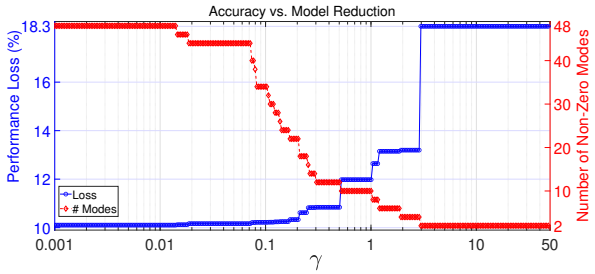

Figure 4: A batch of sparsity weight $\gamma \in [0.001, 50]$, with 300 grid points corresponding to the path of $\mathbf{b}_r^*(\gamma)$, showing a trade-off between performance loss and the number of selected (non-zero) modes or amplitudes with SPDMD.

modes reveal the emergence of warm bubble-like patterns. In particular, for those decaying Koopman modes $\boldsymbol{\phi}_j$ for $j = 3, 5, 7, 9$, they show a clearer warm bubble-like structure dynamics, suggesting these transient modes are useful for understanding the dissipation phase of heavy rainfall events. Meanwhile, the growth Koopman modes $\boldsymbol{\phi}_1$ and $\boldsymbol{\phi}_{11}$ are more correlated with the onset or potential development or growth of heavy rain.

Table 2: Model reduction, cost, and loss as tuned by γ.

Weight γ	Modes #i	Cost $J_\gamma(\mathbf{b}_r^\star)$	Loss $\Pi\%$
0.0010	48	0.1167	10.1060
0.1104	30	0.1191	10.2266
0.1705	22	0.1220	10.3318
0.2632	14	0.1340	10.8274
0.4528	12	0.1343	10.8412
0.9338	10	0.1640	11.9774
1.1190	8	0.1826	12.6415
2.8671	4	0.1990	13.1969
2.9727	2	0.3829	18.3031
50.000	2	0.3829	18.3031

Furthermore, we evaluate the accuracy (i.e., the least-square error) in relation to the model complexity (i.e., the number of selected or reduced modes) using SPDMD in (10). For this, we define the performance loss, that is, the error $J_0(\mathbf{b}_r^\star) = \|\mathbf{Y} - \boldsymbol{\Phi}\mathrm{diag}(\mathbf{b}_r^\star)\mathbf{V}_r\|_{\mathrm{F}}^2$ at the sparse optimal amplitudes $\mathbf{b}_r^\star$, normalized with $J_0(0) = \|\mathbf{Y}\|_{\mathrm{F}}^2$, described as $\Pi\% = 100\sqrt{J_0(\mathbf{b}_r^\star)/J_0(0)}$. The case $\Pi\%$ indicates no loss of modeling by the DMD method, while the case $\Pi\% = 100$ implies another extreme case where no Koopman mode is selected. Fig. 4 illustrates the trade-off between accuracy and model reduction as the sparsity weight $\gamma \in [0.001, 50]$ varies over 300 grid points. It is evident that as the sparsity weight γ increases, the number of non-zero amplitudes $\mathbf{b}_r$ decreases, leading to an increase in performance loss $\Pi\%$ (or decrease in accuracy) and a reduction in the number of modes. Table 2 further details Fig. 4. Reducing the number of humidity ratio modes from 48 to 12 results in only a 0.74% increase in least square error. However, reducing the modes further from 12 to 10 causes a 1.13% performance loss, and from 10 to 4, it worsens by 1.2%. A sharper decline occurs when the number of modes drops from 4 to 2, with a 5.10% performance deterioration, increasing the loss from 13.20% to 18.30%. This significant loss shows that further reduction is undesirable and ineffective. Additionally, increasing the weight from $\gamma = 2.9727$ to $\gamma_{\max} = 50$ has no further effect on mode reduction, and the performance loss stabilizes at 18.30%.

4. Conclusion

This study exploited the KMD and SPDMD to capture the dominant transient modes in terms of the warm bubble-like patterns for short-term SCALE weather simulations on humidity ratio data field. By means of SPDMD, we effectively extracted the transient modes and made a trade-off between the accuracy and the model complexity.

Acknowledgments

This work was supported part by JST Moonshot R&D Grant Number JPMJMS2284.

References

[1] D. L. Hartmann, *Global physical climatology*, vol. 103. Newnes, 2015.

[2] A. Mauroy, I. Mezic, and Y. Susuki, *Koopman operator in systems and control*. Springer, 2020.

[3] J. N. Kutz, S. L. Brunton, B. W. Brunton, and J. L. Proctor, *Dynamic mode decomposition: data-driven modeling of complex systems*. SIAM, 2016.

[4] C. W. Rowley, I. Mezić, S. Bagheri, P. Schlatter, and D. S. Henningson, "Spectral analysis of nonlinear flows," *J. Fluid Mech.*, vol. 641, pp. 115–127, 2009.

[5] Y. Susuki, I. Mezic, F. Raak, and T. Hikihara, "Applied Koopman operator theory for power systems technology," *NOLTA, IEICE*, vol. 7, no. 4, pp. 430–459, 2016.

[6] A. Navarra, J. Tribbia, and S. Klus, "Estimation of Koopman transfer operators for the equatorial Pacific SST," *J. Atm.. Sci.*, vol. 78, no. 4, pp. 1227–1244, 2021.

[7] M. R. Jovanović, P. J. Schmid, and J. W. Nichols, "Sparsity-promoting dynamic mode decomposition," *Physics of Fluids*, vol. 26, no. 2, 2014.

[8] S. Nishizawa, H. Yashiro, T. Yamaura, A. Adachi, Y. Sachiho, Y. Sato, and H. Tomita, "SCALE (scalable computing for advanced library and environment) v5. 3.6 [software]. zenodo," 2020.

[9] Z. Zhang, Y. Susuki, and A. Okazaki, "Extracting transient Koopman modes from short-term weather simulations with sparsity-promoting dynamic mode decomposition," *arXiv preprint arXiv: 2506.14083*, 2025.